Applied Chemical Engineering (2020) Volume 3 Issue 1
doi:10.24294/ace.v3i1.509

ORIGINAL RESEARCH ARTICLE

Photocatalytic oxidation of psychoactive drug Duloxetine: Degradation kinetics, inorganic ions and phytotoxicity evaluation

Sophia Tsoumachidou[1*], Maria Valari[2], Ioannis Poulios[1]

[1]*Laboratory of Physical Chemistry, Department of Chemistry, Aristotle University of Thessaloniki, 54124 Thessaloniki, Greece; E-mail: stsoumac@chem.auth.gr*

[2]*InterBalkan Environment Center, 57200, Lagadas, Greece.*

ABSTRACT

Pharmaceutically active compounds, emerging extensively in ecosystems as pollutants, have become an important environmental and public health issue, since they can contaminate drinking water and pose threat to wildlife and human health. Therefore, efforts should be made in order to establish proper methods for their inactivation or elimination in the environment. The photocatalytic oxidation of psychoactive drug Duloxetine (DLX) has been investigated. In the case of heterogeneous photocatalytic oxidation, the effect of TiO_2 P25 concentration (0.1–1 g L^{-1}), initial concentration of H_2O_2 (0.25–0.2 g L^{-1}) and Fe^{3+} (0.00175–0.014 g L^{-1}) and pH of the solution (3–10) on initial reaction rates were evaluated, while for homogeneous photocatalytic oxidation the effect of the amount of H_2O_2 (0.25–0.2 g L^{-1}) and Fe^{3+} (0.00175–0.014 g L^{-1}) were investigated. Additionally, the conversion of the heteroatoms in the molecule of DLX to inorganic ions (NO_3^-, NH_4^+, SO_4^{2-}) during photocatalytic process has been observed, and phytotoxicity testing, using three plant species, was carried out in order to examine the effect of photocatalytic oxidation on the toxicity of DLX. According to the results presented in this study, both heterogeneous and homogeneous photocatalytic oxidation is an efficient methodology for DLX degradation.

***Keywords*:** Duloxetine; Photocatalytic Oxidation; Psychoactive Drug; Urban Wastewater

ARTICLE INFO

Received 27 April 2020
Accepted 29 May 2020
Available online 9 June 2020

1. Introduction

Pharmaceutical active compounds (PhACs) are turning into an essential ecological and public health issue, because of their expanding use and subsequent release in the aquatic environment and their potential effects on wildlife and humans. Drug residues that have been identified recently in urban surfaces, groundwater and drinking water[1,2], are mostly introduced in the sewage system through excretion of unmetabolized compounds after medical use or inappropriate disposal[3]. However, effluents of wastewater treatment plants (WWTPs) are generally recognized as the major emission pathway of pharmaceuticals into the environment[4], due to the fact that conventional WWTPs are designed to remove solids and nutrients and to reduce the biological oxygen demand of the effluent[5]. Even though, pharmaceuticals usually do not have toxic impact on aquatic organisms, since they are detected at low or very low concentrations (ng to μg per liter), concerns have been raised for chronic exposure, since their continuous input to the environment exceed their degradation rate, acting, thus, as slightly persistent pollutants[6].

Psychoactive compounds are a group of drugs used to treat symptoms of neurological disorders such as depression, schizophrenia, bipolar disorder,

or anxiety disorders. According to Global Burden of Disease Study, jointly published by World Health Organization (WHO) and other groups, neuropsychiatric disorders have emerged as priority health problems worldwide, projected to be the second most frequent disease by 2020[7], while Almeida *et al*. showed that lifetime prevalence of such disorders can reach over 25%[8]. Moreover, according to WHO, around 10% of fully grown persons suffer from such disorders at any point in their lifetime[9]. Many previous studies showed that, exposure of aquatic organisms to psychoactive compounds may affect reproduction[10], endocrine function[11], or photosynthesis[12]. Furthermore, recent studies showed that psychoactive drugs may alter fish and benthic invertebrates behavioral responses[13], and also, induce fish gene expression profiles associated with human idiopathic autism[14].

During the current economic crisis in Greece, the consumption of psychoactive substances has risen significantly, resulting in an increase in their concentration in urban wastewater[15]. The presence of psychoactive substances and/or their metabolites is confirmed, not only in urban wastewater, but also in aquatic plants and animal tissues[16,17], underlining the possible consequences for human health and ecosystems balance. Pollution of European waters by pharmaceuticals is a ubiquitous phenomenon[18,19] and is receiving great attention, as stated in the EU Directive 2013/39/EU19 on priority substances in the field of water policy[20]. Notwithstanding, wastewater management remains an open issue for the members of the European Union, since legislations is incomplete and in need of update[21]. Given the increasing interest about aquatic environment contamination by psychoactive compounds, legislation has recently begun to acknowledge this potential problem in order for environmental regulations to require explicit testing for any PhACs in water bodies.

In order to solve various problems encountered by conventional methods for the degradation of organic species resistant to them, many researchers have turned their attention to a particular group of oxidation techniques called Advanced Oxidation Processes (AOPs). Among AOPs, heterogeneous and homogeneous photocatalytic oxidation has been studied extensively and it has been demonstrated to be an alternative to conventional methods for the removal of organic pollutants from water and air[22,23]. Meanwhile, photocatalytic oxidation has the potential to use solar energy, integrating, in this way, mild energy into environment protection.

The aim of this work was the application of the preceding methods at the degradation of psychoactive drug Duloxetine (DLX), a serotonin norepinephrine reuptake inhibitor (SNRI) widely used for patients with depression and neuropathic pain. The study provides a further insight to oxidation kinetics (i.e. determination of factors affecting oxidation rate) and estimates mineralization degree towards the corresponding oxidation process. In addition, the conversion of the heteroatoms in the molecule of DLX to inorganic ions (NO_3^-, NH_4^+, SO_4^{2-}) during photocatalytic process has been observed, and phytotoxicity testing, using three plant species, was carried out in order to examine the effect of photocatalytic oxidation on the toxicity of DLX.

2. Material and methods

2.1 Reagents

Duloxetine hydrochloride was the product of Sigma-Aldrich and was used as received. NaOH and HCl were used to adjust the pH when necessary. Commercially available TiO_2 catalyst from Evonik, Aeroxide TiO_2 P25 (TiO_2 P25, 70% anatase and 30% routile with BET surface area of 55 ± 15 $m^2\ g^{-1}$) was employed in this study. Iron chloride ($FeCl_3{\cdot}6H_2O$) and hydrogen peroxide (H_2O_2, 30% w/v) were purchased from Alfa Aesar and Panreac Qu ́mica, respectively, and they were used without further purification. Double distilled water was used throughout the experimental processes.

2.2 Experimental set-up and procedures

A thermostated pyrex cell of 0.25 L capacity used as the reaction vessel, was fitted centrally with UV-A or visible light of identical dimensions and geometry, and covered with a black cloth to avoid interactions with ambient light. An Osram Dulux® S blue UV-A lamp (9W/78, 350−400 nm) and an Osram Dulux® S blue lamp (9W/71, 400−550 nm) were used as artificial light sources. The photon flux emitted from the lamps was determined acti-

nometrically using the potassium ferrioxalate [$K_3Fe(C_2O_4)_3 \cdot 3H_2O$] method[24]. The radiation intensities obtained for the UV-A and the visible lamp were $1.268 \cdot 10^{-4}$ E min^{-1} L^{-1} and $0.724 \cdot 10^{-4}$ E min^{-1} L^{-1}, respectively.

In order to check reproducibility of the results, all photocatalytic experiments were performed in duplicate and, in some cases, in triplicate, with the standard deviation never to exceed 5% for degradation experiments and 10% for DOC and inorganic ions analysis.

It must be mentioned that DLX concentration employed in all experiments was substantially higher than the typically one found in environmental samples, in order to assess treatment efficiency within a measurable time scale and accurate determine residual concentrations with the analytical techniques employed in this work.

2.3 Analytical methods

Sample absorbance was scanned in the 200–400 nm wavelength region on a Shimadzu UV-1700 spectrophotometer and changes in the concentration of DLX were monitored via its characteristic absorption band at 289 nm. A Shimadzu V_{CSH} Total Organic Carbon Analyzer was used for following mineralization by measuring the dissolved organic carbon (DOC), while pH was determined with a Mettler Toledo S20 SevenEasy pH meter. Colorimetric determination with spectrophotometric detection with titanium (IV) oxysulfate-sulfuric acid solution according to DIN 38409 H15, a method based on the formation of a yellow complex from the reaction of titanium (IV) oxysulfate with H_2O_2, was used for residual hydrogen determination.

A Shimadzu system, comprising of an LC-10 AD pump, a CTO-10A column oven and a CDD-6A conductivity detector (0.25 μL flow-cell), was used for inorganic anions determination. Anions separation was performed on an Alltech Allsep column preceded by a guard column of the same material, using a mixture of phthalic acid and lithium hydroxide at 1.5 mL min^{-1} constant flow. Temperature of column and conductivity cell was constantly held at 35 ^{o}C and 38 ^{o}C, respectively. Before LC analysis mobile phases were degassed with helium stream. An ion chromatography (IC) unit LC 20 AD (Shimadzu), consisted of an LC-20 pump, a ADsp degasser, a DGU-20A5, a CDD-10 A VP conductivity detector and a CTO-20A oven, was used for inorganic cations identification. Cations separation was held on an IC YK-421 analytical column, with a mobile phase of boric acid, tartaric acid and dipicolinic acid, through adsorption and desorption processes and detected based on their elution time. Before their injection in the column, samples were filtered through a 0.45 mm membrane filter.

2.4 Phytotoxicity evaluation

Phytotoxicity measurements was performed in order to determine photocatalytic efficacy to decrease DLX toxicity, using the standard Phytotoxkit microbiotest, a bioassay based on three species of higher plants: the monocotyl Sorgho (Sorghum saccharatum), the dicotyl garden cress (Lepidium sativum) and the dicotyl mustard (Sinapis alba).

This article measures both the decrease/absence of seed germination and the decrease of roots and/or shoots after 3 days of exposure of the seeds to toxicants or contaminated soils. For this purpose, reference soil (an OECD analogous artificial soil composed of sand, kaolin, peat and pH adjusted with $CaCO_3$) was added in the lower compartment of the test plates and hydrated with the samples, while control tests were prepared using distilled water. The soil surface was flattened and covered by paper filter. Tests were carried out in three replicates for each sample and for each type of plant. The seeds were left in a dark incubator at 25 ^{o}C for 3 days prior to recording and interpretation of results. Digital pictures of the plates were analyzed using Image J v1.49 software (Wayne Rasband, national Institutes of Health, USA). The test results were evaluated comparing the mean number of germinated seeds and the mean root/shoot length for the three replicates in the control and in each examined sample. The percentage effect of the tested effluents on seed germination inhibition (GI), root growth inhibition (RGI) and shoot growth inhibition (SGI) was calculated applying the following formula.

$$\%effect = \frac{A-B}{A} \times 100 \quad (1)$$

where *A* represents the average number of germinated seeds or the average root length in the control water and *B* represents the same parameters for the tested solution.

3. Results and discussion

3.1 Heterogeneous photocatalytic oxidation of DLX

3.1.1 Effect of catalyst's loading

The degradation of an organic compound may be influenced strongly by TiO_2 dosage, since this parameter is an important factor in slurry photocatalytic processes. **Figure 1** depicted the effect of varying the quantity of TiO_2 P25 on the observed initial reaction rate r_o of DLX degradation and mineralization degree. The proper catalyst amounts were added to 0.01 g L^{-1} DLX solutions in natural pH (~5.5) and then irradiated with UV-A light. The pH value falls about 1.5 unit after the photocatalytic process. Preliminary experiments with DLX solution containing TiO_2 in the dark or illuminated DLX solution without the presence of catalyst showed that both illumination and catalyst are essential for the degradation of the drug (data not shown).

The values of the initial degradation rate and mineralization degree in relation to catalyst dosage are depicted in **Figure 1**. The initial reaction rates were calculated by a linear fit of C-t data obtained during the first minutes of illumination, in order to minimize variations resulting in the competitive effects of the intermediate products and pH changes. As it can be seen, the increase of TiO_2 loading from 0.1 to 0.75 g L^{-1} led to an increase in the initial reaction rate. Moreover, DOC was 95.9% reduced after 120 min of illumination, when heterogeneous photocatalytic oxidation was conducted in the presence of 1 g L^{-1} TiO_2 P25. The observed trend can be attributed to the evidence that a catalyst dose increase can provide larger surface area for DLX oxidation and, additionally, may increase the active sites amount that can also provide an enhancement to the photocatalytic efficiency[25]. Nonetheless, above a certain value a slightly decrease in the reaction rate is observed, a behavior similar to our previous studies[26,27], which may be due to a possible aggregation of the catalyst (particle-particle interactions) which result in a loss of surface area available for light-harvesting[28]. Furthermore, there may be an increase in the opacity of the solution leading to a decrease of the light penetration causing the lesser activation of the catalyst resulting in marginal change or even reduced degradation due to the negative contributions of aggregation or reduced energy[25,29].

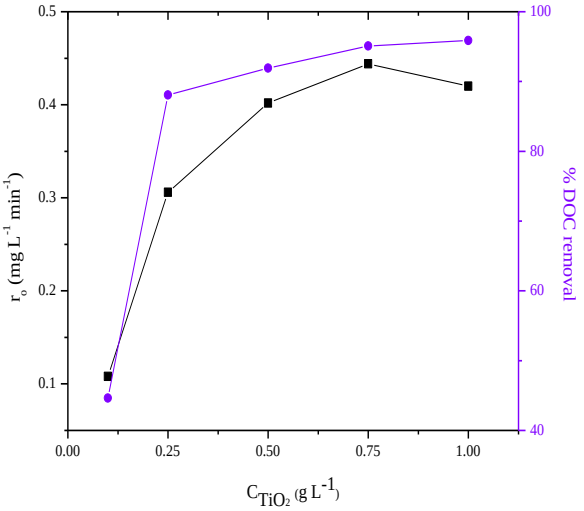

Figure 1. Dependence of the initial reaction rate for constant DLX concentration, r_o, (■) on the concentration of the TiO_2 P25 and DLX mineralization degree (●) at 120 min of photocatalytic process (initial conditions: 0.01 g L^{-1} DLX, pH ≈ 5.5, T = 25 °C, UV-A illumination).

Considering the above, in order to ensure total absorption of efficient photons and avoid excess catalyst, the optimum catalyst dosage must be determined[30]. As shown in **Figure 1**, the optimum value is approximately 0.75 g L^{-1}. Observing that with lower catalyst concentration a good efficiency was obtained and considering the necessity of a good balance between process efficiency and experimental costs, in the following experimental runs, the catalyst dosage was chosen to be 0.25 g L^{-1}.

3.1.2 Effect of electron scavengers

The acceleration of the photocatalytic oxidation by the addition of oxidizing species (e.g. H_2O_2) with the potential to capture the photogenerated electrons is an extensively studied procedure[31]; due to various individual phenomena that are taking place, such as increment of trapped e^-, avoiding, thus, the e^-/h^+ recombination, enhanced $HO^\bullet$ and secondary oxidizing species generation, intermediate compounds oxidation rate increment and reduction of potential problems caused by low O_2 con-

centration decrease[32]. It is established that, H_2O_2 gets a photogenerated electron from the conduction band, promoting, therefore, the charge separation, while, it can also produce $HO^{\bullet}$ via superoxide. However, too high peroxide dosage can promote a negative effect on organic pollutants oxidation, since H_2O_2 is also a semiconductor valence band holes and $HO^{\bullet}$ scavenger. Therefore, as observed in previous studies, the effect of oxidant additives, such as hydrogen peroxide, can be conflicting depending on the amount and the particular experimental conditions[33].

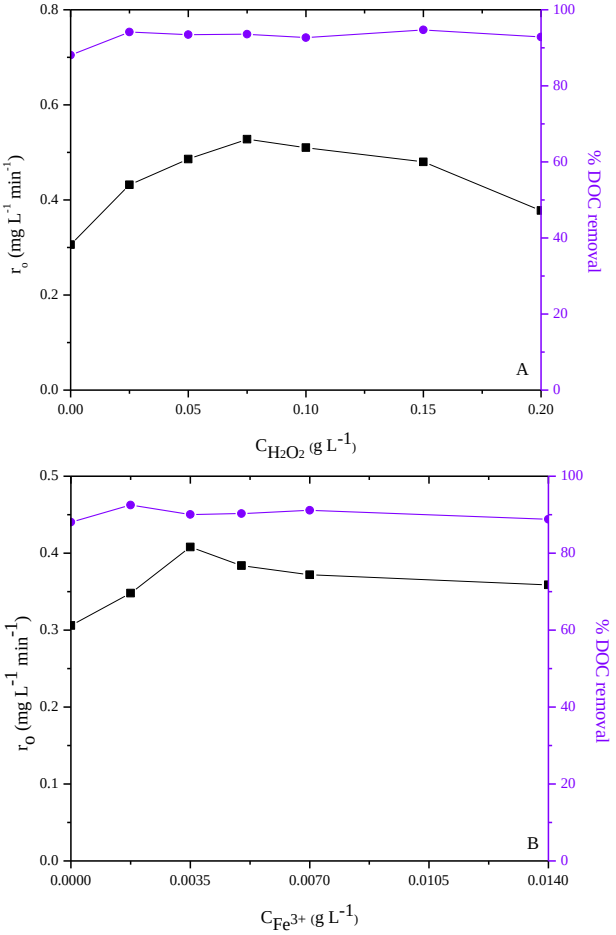

Figure 2. Effect of H_2O_2 **(A)** and ferric ions **(B)** concentration on the initial reaction rate of DLX degradation (■) and DLX mineralization degree (●) at 120 min and 90 min, respectively, of photocatalytic process (initial conditions: 0.01 g Ł$^{-1}$ DLX, 0.25 g Ł$^{-1}$ TiO_2 P25, pH ≈ 5.5, T = 25 °C, UV-A illumination).

In order to investigate H_2O_2 role, photocatalytic experimental runs for the oxidation of 0.01 g Ł$^{-1}$ DLX in the presence of 0.25 g Ł$^{-1}$ TiO_2 P25, were performed with different H_2O_2 dosage and at the natural pH value of drug solutions. **Figure 2A** depicted the effect of H_2O_2 addition on TiO_2-mediated photocatalytic mineralization of DLX. In all H_2O_2-induced experiments presented in **Figure 2A**, over 80% of DLX was eliminated within 20 minutes of reaction. An increase in the concentration of H_2O_2 from 0.025 to 0.075 g Ł$^{-1}$ led to a small increase in the oxidation rate from 0.31 to 0.53 g Ł$^{-1}$ min^{-1}, while higher H_2O_2 dosage resulted to a slightly r_o reduction down to 0.38 g Ł$^{-1}$ min^{-1}, a behavior that has been also obtained in similar studies. Furthermore, mineralization experimental runs showed that DLX dissolved organic carbon was almost 95% reduced after 120 min of illumination for all H_2O_2 concentrations studied.

Metal ions addition has also been proven to increase photocatalytic effectiveness, since they are able to trap, separate and transfer the photogenerated electrons and holes in semiconductors[34]. In an attempt to enhance the efficiency of the TiO_2-induced photocatalytic process, iron in the form of Fe^{3+} was introduced in the reaction vessel prior the beginning of the reaction. The facilitation by Fe^{3+} at DLX degradation and mineralization is shown in **Figure 2B**. The observed enhancing effect could be attributed to interactions between iron species and TiO_2[35], the efficient electron-hole pair separation, since the addition of suitable scavengers can suppress the photocatalytic process efficiency limitation occurred by the recombination of photogenerated electrons and holes. Ferric ions act as a photo-generated e^- or h^+ trap, inhibiting, thus, their recombination and enhancing their lifetimes[25]. Furthermore, Fe^{3+} reduction to Fe^{2+} by a photo-generated e^- in TiO_2 particles can also conduce to the suppression of electron-hole recombination[36].

3.1.3 Effect of solution's pH

The pH of the solution seems to have a significant role in the heterogeneous photocatalytic process efficiency[37,38], since surface charge state and flat band potential, among other catalyst's properties, appear to have a high pH dependence. Additionally, the degradation rate may be enhanced or inhibited by catalyst's surface and organic molecule electrostatic attraction or repulsion[39]. Moreover, the size of TiO_2 particles, the catalyst's interaction with solvent molecules and the type of radicals or intermediates formed during photocatalytic process, may be pH-affected. All aforementioned factors can

affect organic molecules adsorption onto catalyst and, consequently, influence the observed degradation rates[40].

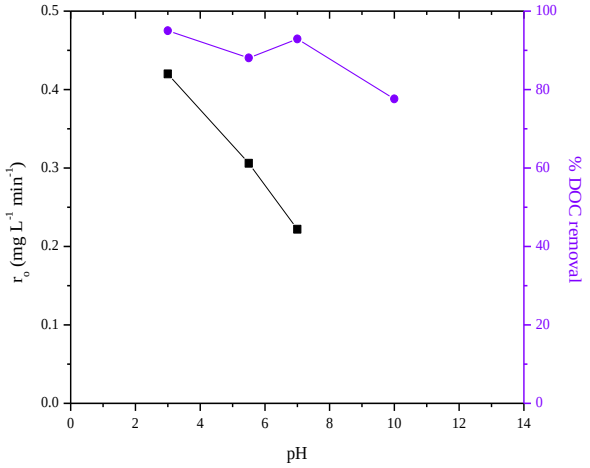

Figure 3. Effect of pH on the initial reaction rate of DLX degradation (■) and DLX mineralization degree (●) at 120 min of photocatalytic process (initial conditions: 0.01 g Ł$^{-1}$ DLX, 0.25 g Ł$^{-1}$ TiO_2 P25, pH ≈ 5.5, T = 25 °C, UV-A illumination).

Solution's initial pH impact on photocatalytic oxidation was studied by performing the experiments with 0.25 g Ł$^{-1}$ TiO_2 P25 in 0.01 g Ł$^{-1}$ DLX solution, under UV-A illumination and adjusting the solution pH from acidic values to alkaline ones; the results on degradation rate of DLX and its DOC reduction after 120 min of illumination are demonstrated in **Figure 3.** Usually, at pH values below its pK_a, an organic compound exists as neutral species or in a cationic form, whereas above this value, gets a negative charge. For that reason and considering that at this area the catalyst's surface is positively charged, it is not likely to achieve great electrostatic attractions between the surface of the catalyst and the organic molecules. With pH increment, substance's negative charging is getting stronger and, therefore, the electrostatic interactions are getting more remarkable, causing, this way, an enhancement in the photocatalytic efficiency[41]. In this case, as it can be seen from **Figure 3**, when the pH value decreases from 7 to 3 an increase of the DLX degradation rate is observed. Although opposite to the expected, this phenomena can be explained by the fact that DLX has be found in previous studies to be unstable in acidic media[42,43].

3.2 Homogeneous photocatalytic oxidation of DLX

Fenton reagent is a drawing attention oxidative system, since hydrogen peroxide is wieldy and environmental safe and iron is a very abundant and non-toxic material[44]. Considering its high ability to generate HO$^{\bullet}$ in a very simple way, as a result of H_2O_2 decomposition by Fe^{2+} in acidic medium, Fenton method has been widely applied for organic compounds oxidation[45]. The advantages of photo-Fenton process are the safe and environmentally-benign nature of reagents and relatively simple operating principles as well as short reaction time and the absence of mass transfer limitations[46]. In addition, with the use of light (UV-A or visible, artificial or natural) the process can be catalytic, since the photo-reduction of Fe^{3+} to Fe^{2+} produces additional hydroxyl radicals and leads to the catalyst regeneration (Equation (3))[45].

$$Fe^{2+} + H_2O_2 \rightarrow Fe^{3+} + OH^- + HO^{\bullet} \quad (2)$$

$$Fe^{3+} + H_2O + h\nu \rightarrow Fe^{2+} + H^+ + HO^{\bullet} \quad (3)$$

One of the main parameters that influence the Fenton and photo-Fenton processes is the iron amount. In the majority of cases, the photocatalytic effect is enhanced when the iron concentration is increased, since more hydroxyl radicals' production is obtained[47–49].

As the iron concentration increases, the regeneration of Fe^{2+} from Fe^{3+} results in the rapid production of additional HO$^{\bullet}$[47]. However, with too high ferric amount in the solution, dark zones can be generated in the photoreactor, since the incident ray is attenuated too strongly along the optical pathlength, reducing, for that reason, the process effectiveness. Moreover, although more radicals can be produced (Equation (3)), they can be scavenged by reacting with other ferrous ions, which lead to the reduction of their amount[50].

As it can be seen in **Figure 4A**, the increment of ferric ions from 0.00175 to 0.014 g Ł$^{-1}$ led to an increase on the photo-Fenton induced mineralization percentage of DLX, from 78.7 to 94.8% when the solution was illuminated for 120 min with UV-A light and from 70.8 to 94% under visible illumination. In all homogeneous photocatalytic experimental runs the pH was low enough (pH = 3.2–3.3), since iron precipitates at higher pH.

Iron concentration has proven to be a signifi-

cant parameter, not only because it can affect the capital costs, but also the operating costs, since shorter reaction times are required[51]. In the presence of high iron amount, the issue of the iron-separation step at the end of the photocatalytic process appears. Consequently, it is considered critical to choose the proper iron concentration in order to achieve as short reaction time as possible, and at the same time not to exceed the limits defined by the direct discharge to biological municipal WWTPs regulations (different amounts are permitted in the EU, USA, Switzerland, etc.)[52].

It should be mentioned that DLX organic load reduction was found to be always faster in the early stages of the reaction than in the later ones, maybe due to the fact that iron ions catalyses H_2O_2 to produce $HO^{\bullet}$ quickly, in the first stages of the photocatalytic oxidation[52].

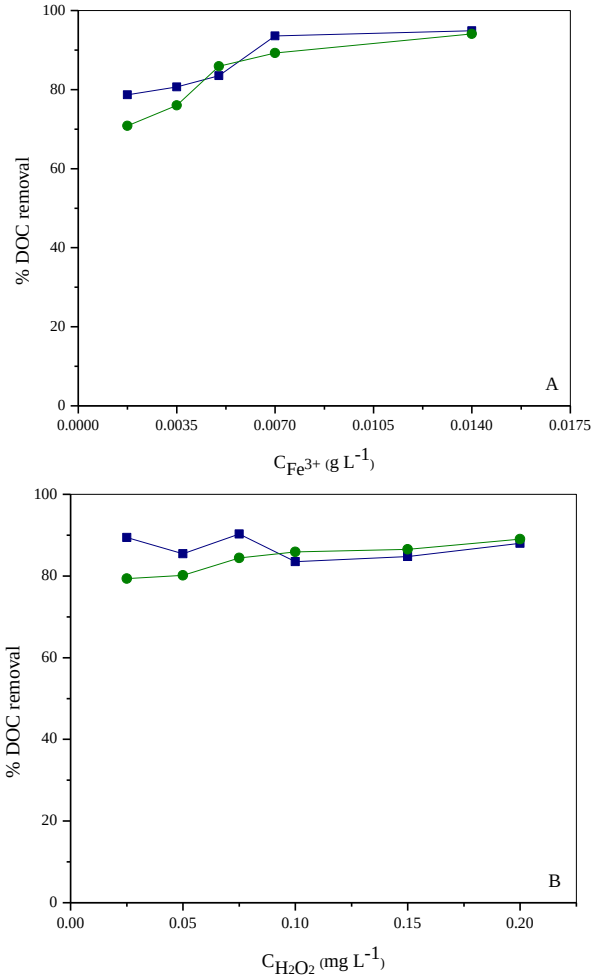

Figure 4. Influence of ferric ions **(A)** and H_2O_2 **(B)** concentration on the degree of mineralization of DLX under UV-A (■) and visible (●) irradiation after 120 min (initial conditions: **(A)** 0.01 g L^{-1} DLX, 0.1 g L^{-1} H_2O_2, pH ≈ 3.3, T = 25 °C; **(B)** 0.01 g L^{-1} DLX, 0.005 g L^{-1} Fe^{3+}, pH ≈ 3.3, T = 25 °C.

The influence of H_2O_2 concentration was investigated by several previous studies[47,54], with the main findings to be that neither too low H_2O_2 amount nor too high may be applied, since in the first case a Fenton reaction rate reduction is occurred, while, in the second H_2O_2 competes successfully for $HO^{\bullet}$ and becomes decomposed into molecular oxygen and water, while oxidizing the pollutant. However, in general, there is a ther broad concentration interval between both extremes, where none of those two phenomena occurs[49].

As shown in **Figure 4B**, the use of extra H_2O_2 dosage did not result to any remarkable improvement in both UV-A and visible-irradiated process efficiency of DLX photo-Fenton mineralization. Even though, with the oxidant decomposition to be enhanced, a higher amount of $HO^{\bullet}$ is expected, its increment can provide an adverse effect by slowing down the oxidation process, since the competition interactions are enhanced in the case of H_2O_2 excess[55]; mainly the recombination of the produced $HO^{\bullet}$, as well as their recombination with H_2O_2, contributing to the $HO^{\bullet}$ scavenging capacity (Equations (4)–(6))[47,54].

$$HO^{\bullet} + HO^{\bullet} \rightarrow H_2O_2 \quad (4)$$

$$H_2O_2 + HO^{\bullet} \rightarrow H_2O + HO_2^{\bullet} \quad (5)$$

$$HO_2^{\bullet} + HO^{\bullet} \rightarrow H_2O + O_2 \quad (6)$$

3.3 Inorganic Ions

Temporal profiles of sulfur (released as sulfate ions) and inorganic nitrogen (i.e. nitrates, nitrites and ammonium ions) released during heterogeneous and homogeneous photocatalytic mineralization of DLX are shown in **Figure 5**. Profiles do not show actual concentrations but they correspond to the percentage of the theoretical amount of sulfur or nitrogen initially present in the molecule.

The heteroatoms contained in the organic compounds are readily converted to inorganic ions that remain in the liquid phase. In some cases, photooxidation of nitrogen is relatively slow and the mineralization of organic pollutants containing nitrogen seems to be complex, since nitrate, nitrite, ammonium ions and free nitrogen are formed[56]. As it can be seen in **Figure 5A**, in the first 30 min of

heterogeneous photocatalytic oxidation only 25% of organic nitrogen has converted into inorganic, while total conversion occurred after 120 min of process. In the case of homogeneous photocatalytic mineralization, a complete conversion has not achieved, but almost 70% of organic nitrogen was converted after 120 min (**Figure 5B**).

On the other hand, high percentage of organic sulfur is converted to inorganic, for both processes, while with photo-Fenton-induced oxidation almost total amount of sulfur is converted to inorganic within the first 30 min of reaction. The decrease of S^- amount, in the case of homogeneous photocatalytic oxidation, may be due to the fact that iron forms a mixture of $FeSO_4^+$ and $Fe(SO_4)_2^-$ complexes in the presence of sulfur[57].

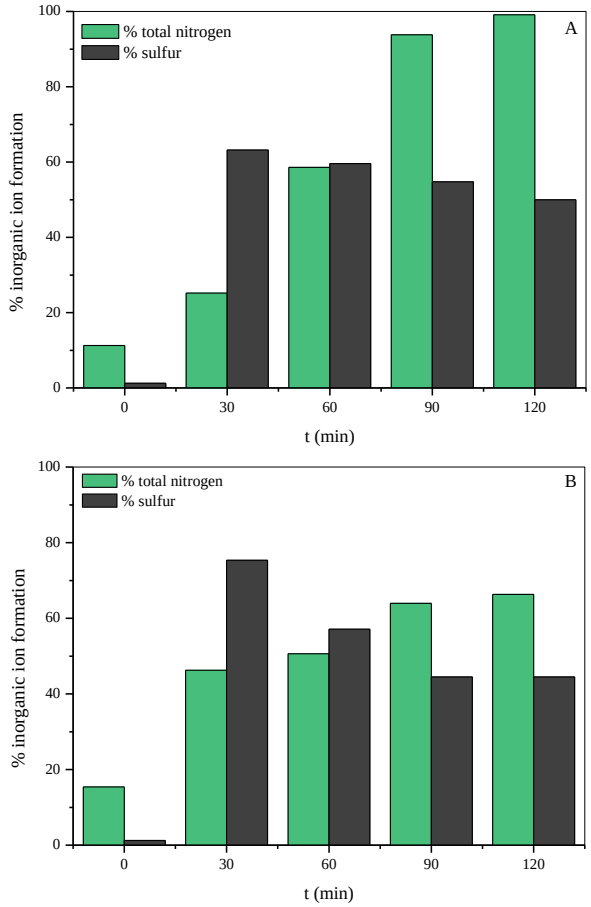

Figure 5. Release of inorganic anions during heterogeneous **(A)** and homogeneous **(B)** photocatalytic mineralization of DLX (initial conditions: (A) 0.01 g L^{-1} DLX, 0.25 g L^{-1} TiO_2 P25, 0.1 g L^{-1} H_2O_2, pH ≈ 5.5, T = 25 °C, UV-A illumination; (B) 0.01 g L^{-1} DLX, 0.007 g L^{-1} Fe^{3+}, 0.1 g L^{-1} H_2O_2, pH ≈ 3.3, T = 25 °C, UV-A illumination).

3.4 Phytotoxicity evaluation

For the investigation of the effect of the TiO_2 photocatalytic process on DLX phytototoxicity, samples of the initial drug solution (raw DLA) and at the end of the process (treated DLX) were selected. It should be noted that there were not any inhibition effects by the H_2O_2, since residual hydrogen peroxide was measured during photocatalytic oxidation and found to be totally eliminated after the reaction. The effects of DLX samples on the plants are depicted in **Figure 6** and they are expressed as root growth inhibition (RGI), shoot growth inhibition (SGI) and seed germination inhibition (GI).

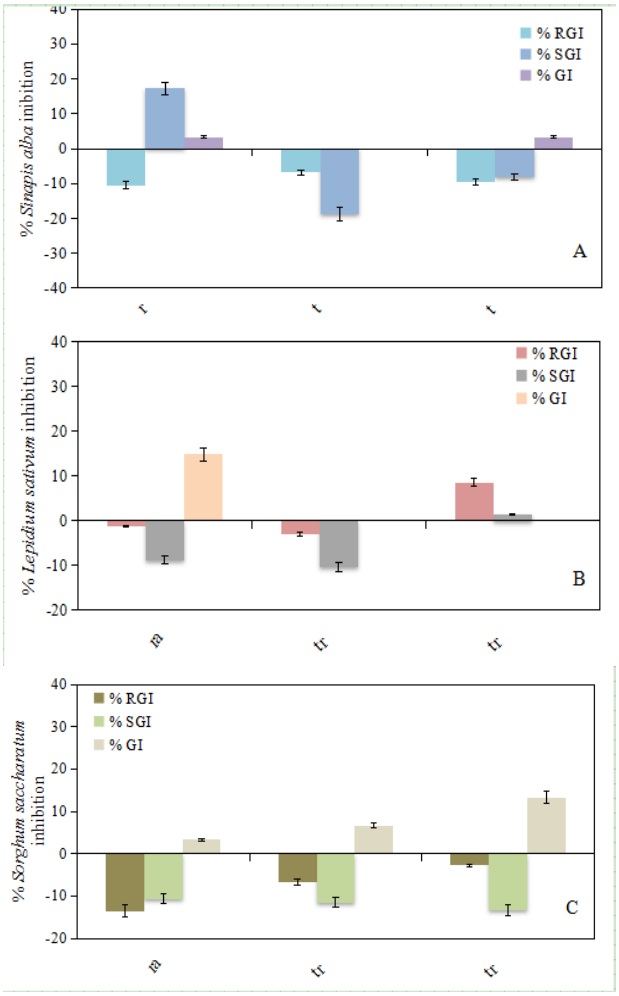

Figure 6. Inhibition effect (%) of DLX before and after treatment with heterogeneous (initial conditions: 0.01 g L^{-1} DLX, 0.25 g L^{-1} TiO_2 P25, 0.1 g L^{-1} H_2O_2, pH ≈ 5.5, T = 25 °C) and homogeneous (initial conditions: 0.01 g L^{-1} DLX, 0.007 g L^{-1} Fe^{3+}, 0.1 g L^{-1} H_2O_2, pH ≈ 3.3, T = 25 °C) photocatalytic oxidation on Sinapis alba **(A)**, Lepidium sativum **(B)**, Sorghum saccharatum **(C)**, under 120 min of UV-A illumination.

As it can be seen from **Figure 6A**, both TiO_2 and photo-Fenton-induced photocatalytic processes improved the phyto-compatibility of DLX, since exposure to the treated solutions affected the soot length of Sinapis alba. The raw DLX solution ex-

erted higher toxicity to the above species as it brought on 17.3% shoot growth inhibition. Furthermore, the seed germination of Lepidium sativum was affected, reaching 14.8% after incubation with raw DLX and total toxicity elimination with both treated solutions (**Figure 6B**).

On the contrary, root and shoot growth germination of Lepidium sativum was negatively affected to photo-Fenton-treated solution exposure, since raw DLX exerted no toxicity to the above parameters, while the treated solution brought a toxic effect of 8.6 and 1.5%, respectively. This observation indicates the need for further photocatalytic processing of DLX, since, apparently, the metabolites that are formed during drug's degradation are more toxic than the parent compound. The same conclusion is derived from **Figure 6C**, where it can be seen that the toxic effect at seed germination of Sorghum saccharatum increased from 3.3%, that was after the exposure to raw DLW, to 6.7 and 13.3% after incubation with treated DLX (heterogeneous and homoegeneous photocatalytic oxidation, respectively).

4. Conclusions

In the present work the photocatalytic oxidative degradation of DLX, a psychoactive drug detected in urban wastewater, has been demonstrated.

With the use of TiO_2 P25 as photocatalyst under UV-A illumination, quantitative mineralization of the organic molecule occur after 2 hours, while as the catalyst dosage increased the initial reaction rate of the drug degradation increased.

In all experimental runs that H_2O_2 was added in the drug solution over 80% of DLX was eliminated within 20 minutes of reaction. An increase in the concentration of H_2O_2 led to a small increase in the reaction rate of oxidation, while a higher concentration of H_2O_2 resulted to a slightly reaction rate reduction. Moreover, mineralization experiments showed that DOC of DLX was almost 95% reduced after 120 min of illumination for all H_2O_2 concentrations studied.

No remarkable enhancement was obtained by the attempt to enhance the efficiency of the TiO_2-induced heterogeneous photocatalytic process by introducing Fe^{3+} in the reaction solution. The study of the effect of drug solution's pH showed that the higher degradation rate occurred at pH 3.

In the case of homogeneous photocatalytic oxidation, the increment of ferric ions led to an increase of DLX mineralization percentage in both UV-A and visible-irradiated process efficiency. On the other hand, the use of extra H_2O_2 dosage did not result to any remarkable improvement in DLX photo-Fenton-induced mineralization.

Inorganic ions formation analysis showed that total organic nitrogen was converted into inorganic after 120 min of heterogeneous photocatalytic oxidation, while in the case of homogeneous process, almost 70% of organic nitrogen was converted after the same illumination time. On the other hand, high percentage of organic sulfur was converted to inorganic, for both processes, while with photo-Fenton-induced oxidation almost total amount of sulfur is converted to inorganic within the first 30 min of reaction.

Phytotoxicity evaluation showed that both TiO_2 and photo-Fenton-induced photocatalytic processes improved the phyto-compatibility of DLX, since exposure to the treated DLX solutions affected the soot length of *Sinapis alba*. Moreover, the seed germination of *Lepidium sativum* was affected, achieving total toxicity elimination with both treated solutions. On the other hand, root and shoot growth germination was negatively affected to photo-Fenton-treated solution exposure, since raw DLX exerted no toxicity to the above parameters, while the treated solution brought a toxic effect of 8.6 and 1.5%, respectively. Additionally, the toxic effect at seed germination of *Sorghum saccharatum* increased after incubation with treated DLX. According to the above, the need for further photocatalytic processing of DLX is required, since, apparently, the metabolites that are formed during drug's degradation are more toxic than the parent compound.

Conflict of interest

The authors declare that they have no conflict of interest.

Acknowledgements

This research project was funded by State Scholarships Foundation (IKY), through IKY Fellowships of Excellence for Postgraduate Studies in Greece-Siemens Program.

References

1. Hofman-Caris CHM, Siegers WG, Van de Merlen K, *et al*. Removal of pharmaceuticals from WWTP effluent: Removal of EFOM followed by advanced oxidation. Chemical Engineering Journal 2017; 327 (Supplement C): 514–521. doi: https://doi.org/10.1016/j.cej.2017.06.154.
2. Pereira AMPT, Silva LJG, Laranjeiro CSM, *et al*. Human pharmaceuticals in Portuguese rivers: The impact of water scarcity in the environmental risk. Science of the Total Environment 2017; 609 (Supplement C): 1182–1191. doi: https://doi.org/10.1016/j.scitotenv.2017.07.200.
3. Xekoukoulotakis NP, Xinidis N, Chroni M, *et al*. UV-A/TiO_2 photocatalytic decomposition of erythromycin in water: Factors affecting mineralization and antibiotic activity. Catalysis Today 2010; 151(1): 29–33. doi: http://dx.doi.org/10.1016/j.cattod.2010.01.040.
4. Ramirez AJ, Brain RA, Usenko S, *et al*. Occurrence of pharmaceuticals and personal care products in fish: Results of a national pilot study in the United States. Environmental Toxicology and Chemistry 2009; 28 (12): 2587–2597. doi: 10.1897/08-561.1.
5. Bu Q, Shi X, Yu G, *et al*. Pay attention to non-wastewater emission pathways of pharmaceuticals into environments. Chemosphere 2016; 165 (Supplement C): 515–518. doi: https://doi.org/10.1016/j.chemosphere.2016.09.078.
6. Puckowski A, Mioduszewska K, Łukaszewicz P, *et al*. Bioaccumulation and analytics of pharmaceutical residues in the environment: A review. Journal of Pharmaceutical and Biomedical Analysis 2016; 127 (Supplement C): 232–255. doi: https://doi.org/10.1016/j.jpba.2016.02.049.
7. Menken M, Munsat TL, Toole JF. The global burden of disease study: Implications for neurology. Archives of Neurology 2000; 57(3): 418–420. doi: 10.1001/archneur.57.3.418.
8. Almeida N, Mari JD, Coutinho E, *et al*. Brazilian multicentric study of psychiatric morbidity — Methodological features and prevalence estimates. British Journal of Psychiatry 1997; 171: 524–529. doi: 10.1192/bjp.171.6.524.
9. Saraceno B. The WHO World Health Report 2001 on mental health. Epidemiologia e Psichiatria Sociale 2002; 11(2): 83–87. doi: 10.1017/s1121189x00005546.
10. Brooks BW, Turner PK, Stanley JK, *et al*. Waterborne and sediment toxicity of fluoxetine to select organisms. Chemosphere 2003; 52(1): 135–142. doi: https://doi.org/10.1016/S0045-6535(03)00103-6.
11. Van der Ven K, Keil D, Moens LN, *et al*. Effects of the antidepressant mianserin in zebrafish: Molecular markers of endocrine disruption. Chemosphere 2006; 65(10): 1836–1845. doi: https://doi.org/10.1016/j.chemosphere.2006.03.079.
12. Escher BI, Bramaz N, Richter M, *et al*. Comparative ecotoxicological hazard assessment of beta-blockers and their human metabolites using a mode-of-action-based test battery and a QSAR approach. Environmental Science & Technology 2006; 40(23): 7402–7408. doi: 10.1021/es052572v.
13. Rosi-Marshall EJ, Snow D, Bartelt-Hunt SL, *et al*. A review of ecological effects and environmental fate of illicit drugs in aquatic ecosystems. Journal of Hazardous Materials 2015; 282: 18–25. doi: https://doi.org/10.1016/j.jhazmat.2014.06.062.
14. Thomas MA, Klaper RD. Psychoactive pharmaceuticals induce fish gene expression profiles associated with human idiopathic autism. PLoS ONE 2012; 7(6): e32917. doi: 10.1371/journal.pone.0032917.
15. Thomaidis NS, Gago-Ferrero P, Ort C, *et al*. Reflection of socioeconomic changes in wastewater: Licit and illicit drug use patterns. Environmental Science & Technology 2016; 50(18): 10065–10072. doi: 10.1021/acs.est.6b02417.
16. Rodayan A, Afana S, Segura PA, *et al*. Linking drugs of abuse in wastewater to contamination of surface and drinking water. Environmental Toxicology and Chemistry 2016; 35(4): 843–849. doi: 10.1002/etc.3085.
17. Chu S, Metcalfe CD. Analysis of paroxetine, fluoxetine and norfluoxetine in fish tissues using pressurized liquid extraction, mixed mode solid phase extraction cleanup and liquid chromatography — tandem mass spectrometry. Journal of Chromatography A 2007; 1163(1): 112–118. doi: http://dx.doi.org/10.1016/j.chroma.2007.06.014.
18. Tiedeken EJ, Tahar A, McHugh B, *et al*. Monitoring, sources, receptors, and control measures for three European Union watch list substances of emerging concern in receiving waters — A 20 year systematic review. Science of the Total Environment 2017; 574 (Supplement C): 1140–1163. doi: https://doi.org/10.1016/j.scitotenv.2016.09.084.
19. Barbosa MO, Moreira NFF, Ribeiro AR, *et al*. Occurrence and removal of organic micropollutants: An overview of the watch list of EU Decision 2015/495. Water Research 2016; 94 (Supplement C): 257–279. doi: https://doi.org/10.1016/j.watres.2016.02.047.
20. EU. European Union: Directive 2013/39/EU of the European Parliament and of the Council of 12 August 2013 amending Directives 2000/60/EC and 2008/105/EC as regards priority substances in the field of water policy. Official Journal of the European Union 2013; L226: 1–17.
21. Kelessidis A, Stasinakis AS. Comparative study of the methods used for treatment and final disposal of sewage sludge in European countries. Waste Management 2012; 32(6): 1186–1195. doi:

https://doi.org/10.1016/j.wasman.2012.01.012.
22. Thakur M, Sharma G, Ahamad T, *et al*. Efficient photocatalytic degradation of toxic dyes from aqueous environment using gelatin-Zr(IV) phosphate nanocomposite and its antimicrobial activity. Colloids and Surfaces B: Biointerfaces 2017; 157 (Supplement C): 456–463. doi: https://doi.org/10.1016/j.colsurfb.2017.06.018.
23. Bogatu C, Perniu D, Sau C, *et al*. Ultrasound assisted sol-gel TiO_2 powders and thin films for photocatalytic removal of toxic pollutants. Ceramics International 2017; 43(11): 7963–7969. doi: https://doi.org/10.1016/j.ceramint.2017.03.054.
24. Braun AM, Maurette MT, Oliveros E. Photochemical Technology. Chichester: John Wiley & Sons Wiley; 1991.
25. Sriwichai S, Ranwongsa H, Wetchakun K, *et al*. Effect of iron loading on the photocatalytic performance of Bi_2WO_6 photocatalyst. Superlattices and Microstructures 2014; 76 (Supplement C): 362–375. doi: https://doi.org/10.1016/j.spmi.2014.10.014.
26. Tsoumachidou S, Velegraki T, Antoniadis A, *et al*. Greywater as a sustainable water source: A photocatalytic treatment technology under artificial and solar illumination. Journal of Environmental Management 2017; 195: 232–241. doi: 10.1016/j.jenvman.2016.08.025.
27. Tsoumachidou S, Velegraki T, Poulios I. TiO_2 photocatalytic degradation of UV filter para-aminobenzoic acid under artificial and solar illumination. Journal of Chemical Technology and Biotechnology 2016; 91 (6): 1773–1781. doi: 10.1002/jctb.4768.
28. Sakthivel S, Neppolian B, Shankar MV, *et al.* Solar photocatalytic degradation of azo dye: comparison of photocatalytic efficiency of ZnO and TiO_2. Solar Energy Materials and Solar Cells 2003; 77(1): 65–82. doi: 10.1016/S0927-0248(02)00255-6.
29. Babuponnusami A, Muthukumar K. A review on Fenton and improvements to the Fenton process for wastewater treatment. Journal of Environmental Chemical Engineering 2014; 2 (1): 557–572. doi: https://doi.org/10.1016/j.jece.2013.10.011.
30. Gaya UI, Abdullah AH. Heterogeneous photocatalytic degradation of organic contaminants over titanium dioxide: A review of fundamentals, progress and problems. Journal of Photochemistry and Photobiology C: Photochemistry Reviews 2008; 9(1): 1–12. doi: https://doi.org/10.1016/j.jphotochemrev.2007.12.003.
31. Liu T, Li X, Yuan X, *et al*. Enhanced visible-light photocatalytic activity of a TiO_2 hydrosol ed by H_2O_2: Surface complexation and kinetic modeling. Journal of Molecular Catalysis A: Chemical 2016; 414 (Supplement C): 122–129. doi: https://doi.org/10.1016/j.molcata.2016.01.011.
32. Boroski M, Rodrigues AC, Garcia JC, *et al*. Combined electrocoagulation and TiO_2 photoassisted treatment applied to wastewater effluents from pharmaceutical and cosmetic industries. Journal of Hazardous Materials 2009; 162(1): 448–454. doi: https://doi.org/10.1016/j.jhazmat.2008.05.062.
33. Rajeshwar K, Osugi ME, Chanmanee W, *et al*. Heterogeneous photocatalytic treatment of organic dyes in air and aqueous media. Journal of Photochemistry and Photobiology C: Photochemistry Reviews 2008; 9(4): 171–192. doi: https://doi.org/10.1016/j.jphotochemrev.2008.09.001.
34. Rincón AG, Pulgarin C. Absence of E. coli regrowth after Fe^{3+} and TiO_2 solar photoassisted disinfection of water in CPC solar photoreactor. Catalysis Today 2007; 124(3): 204–214. doi: http://dx.doi.org/10.1016/j.cattod.2007.03.039.
35. Nahar MS, Hasegawa K, Kagaya S, *et al*. Adsorption and aggregation of Fe(III)–hydroxy complexes during the photodegradation of phenol using the iron-added-TiO_2 combined system. Journal of Hazardous Materials 2009; 162(1): 351–355. doi: http://dx.doi.org/10.1016/j.jhazmat.2008.05.046.
36. Měánková H, Mailhot G, Jirkovský J, *et al*. Effect of iron speciation on the photodegradation of Monuron in combined photocatalytic systems with immobilized or suspended TiO_2. Environmental Chemistry Letters 2009; 7(2): 127–132. doi: 10.1007/s10311-008-0145-2.
37. Mir NA, Haque MM, Khan A, *et al*. Photocatalytic degradation of herbicide Bentazone in aqueous suspension of TiO_2: Mineralization, identification of intermediates and reaction pathways. Environmental Technology 2014; 35(4): 407–415. doi: 10.1080/09593330.2013.829872.
38. Lin Y, Ferronato C, Deng N, *et al*. Study of benzylparaben photocatalytic degradation by TiO_2. Applied Catalysis B: Environmental 2011; 104(3): 353–360. doi: https://doi.org/10.1016/j.apcatb.2011.03.006.
39. Helali S, Dappozze F, Horikoshi S, *et al*. Kinetics of the photocatalytic degradation of methylamine: Influence of pH and UV-A/UV-B radiant fluxes. Journal of Photochemistry and Photobiology A: Chemistry 2013; 255 (Supplement C): 50–57. doi: https://doi.org/10.1016/j.jphotochem.2012.12.022.
40. Tizaoui C, Mezughi K, Bickley R. Heterogeneous photocatalytic removal of the herbicide clopyralid and its comparison with UV/H_2O_2 and ozone oxidation techniques. Desalination 2011; 273(1): 197–204. doi: https://doi.org/10.1016/j.desal.2010.11.036.
41. Ahmed S, Rasul MG, Martens WN, *et al*. Heterogeneous photocatalytic degradation of phenols in wastewater: A review on current status and developments. Desalination 2010; 261(1-2): 3–18. doi: 10.1016/j.desal.2010.04.062.
42. Datar PA, Waghmare RU. Development and validation of an analytical method for the stability of duloxetine hydrochloride. Journal of Taibah University for Science 2014; 8(4): 357–63. doi: https://doi.org/10.1016/j.jtusci.2014.06.001.
43. Sinha VR, Kumria AR, Bhinge JR. Stress Degradation Studies on Duloxetine Hydrochloride and De-

velopment of an RP-HPLC Method for its Determination in Capsule Formulation. Journal of Chromatographic Science 2009; 47(7): 589–593.
44. Carneiro PA, Nogueira RFP, Zanoni MVB. Homogeneous photodegradation of CI Reactive Blue 4 using a photo-Fenton process under artificial and solar irradiation. Dyes and Pigments 2007; 74(1): 127–132. doi: 10.1016/j.dyepig.2006.01.022.
45. Baba Y, Yatagai T, Harada T, *et al*. Hydroxyl radical generation in the photo-Fenton process: Effects of carboxylic acids on iron redox cycling. Chemical Engineering Journal 2015; 277: 229–241. doi: 10.1016/j.cej.2015.04.103.
46. Mirzaei A, Chen Z, Haghighat F, *et al*. Removal of pharmaceuticals from water by homo/heterogonous Fenton-type processes — A review. Chemosphere 2017; 174 (Supplement C): 665–688. doi: https://doi.org/10.1016/j.chemosphere.2017.02.019.
47. Abdessalem AK, Bellakhal N, Oturan N, *et al*. Treatment of a mixture of three pesticides by photo- and electro-Fenton processes. Desalination 2010; 250 (1): 450–455. doi: 10.1016/j.desal.2009.09.072.
48. Tsoumachidou S, Lambropoulou D, Poulios I. Homogeneous photocatalytic oxidation of UV filter para-aminobenzoic acid in aqueous solutions. Environmental Science and Pollution Research 2017; 24 (2): 1113–1121. doi: 10.1007/s11356-016-7434-2.
49. Malato S, Fernandez-Ibanez P, Maldonado MI, *et al*. Decontamination and disinfection of water by solar photocatalysis: Recent overview and trends. Catalysis Today 2009; 147(1): 1–59. doi: 10.1016/j.cattod.2009.06.018.
50. Xu X, Li X, Li X, *et al*. Degradation of melatonin by UV, UV/H_2O_2, Fe^{2+}/H_2O_2 and UV/Fe^{2+}/H_2O_2 processes. Separation and Purification Technology 2009; 68(2): 261–266. doi: 10.1016/j.seppur.2009.05.013.
51. Ioannou LA, Fatta-Kassinos D. Solar photo-Fenton oxidation against the bioresistant fractions of winery wastewater. Journal of Environmental Chemical Enginneering 2013; (1): 703–712.
52. Gernjak W, Krutzler T, Glaser A, *et al*. Photo-Fenton treatment of water containing natural-phenolic pollutants. Chemosphere 2003; 50(1): 71–78. doi: 10.1016/S0045-6535(02)00403-4.
53. Yang M, Hu J, Ito K. Characteristics of Fe^{2+}/H_2O_2/UV oxidization process. Environmental Technology 1998; 19(2): 183–191. doi: 10.1080/09593331908616670.
54. Navarro S, Fenoll J, Vela N, *et al*. Removal of ten pesticides from leaching water at pilot plant scale by photo-Fenton treatment. Chemical Engineering Journal 2011; 167(1): 42–49. doi: 10.1016/j.cej.2010.11.105.
55. Doumic LI, Soares PA, Ayude MA, *et al*. Enhancement of a solar photo-Fenton reaction by using ferrioxalate complexes for the treatment of a synthetic cotton-textile dyeing wastewater. Chemical Engineering Journal 2015; 277: 86–96. doi: 10.1016/j.cej.2015.04.074.
56. Nohara K, Hidaka H, Pelizzetti Z, *et al*. Processes of formation of NH_4^+ and NO_3^- ions during the photocatalyzed oxidation of N-containing compounds at the titania/water interface. Journal of Photochemistry and Photobiology A: Chemistry 1997; 102(2): 265–272. doi: https://doi.org/10.1016/S1010-6030(96)04478-4.
57. Pignatello JJ, Oliveros E, MacKay A. Advanced oxidation processes for organic contaminant destruction based on the Fenton reaction and related chemistry. Critical Reviews in Environmental Science and Technology 2006; 36(1): 1–84. doi: 10.1080/10643380500326564.